Published in final edited form as:
J Comp Neurol. 2011 August 1; 519(11): 2175–2192. doi:10.1002/cne.22623.

Morphologic Integration of Hilar Ectopic Granule Cells into Dentate Gyrus Circuitry in the Pilocarpine Model of Temporal Lobe Epilepsy

Michael C. Cameron, **Ren-Zhi Zhan**, and **J. Victor Nadler***
Department of Pharmacology and Cancer Biology and Department of Neurobiology, Duke University Medical Center, Durham, North Carolina 27710

Abstract

After pilocarpine-induced status epilepticus, many granule cells born into the postseizure environment migrate aberrantly into the dentate hilus. Hilar ectopic granule cells (HEGCs) are hyperexcitable and may therefore increase circuit excitability. This study determined the distribution of their axons and dendrites. HEGCs and normotopic granule cells were filled with biocytin during whole-cell patch clamp recording in hippocampal slices from pilocarpine-treated rats. The apical dendrite of 86% of the biocytin-labeled HEGCs extended to the outer edge of the dentate molecular layer. The total length and branching of HEGC apical dendrites that penetrated the molecular layer were significantly reduced compared with apical dendrites of normotopic granule cells. HEGCs were much more likely to have a hilar basal dendrite than normotopic granule cells. They were about as likely as normotopic granule cells to project to CA3 pyramidal cells within the slice, but were much more likely to send at least one recurrent mossy fiber into the molecular layer. HEGCs with burst capability had less well-branched apical dendrites than nonbursting HEGCs, their dendrites were more likely to be confined to the hilus, and some exhibited dendritic features similar to those of immature granule cells. HEGCs thus have many paths along which to receive synchronized activity from normotopic granule cells and to transmit their own hyperactivity to both normotopic granule cells and CA3 pyramidal cells. They may therefore contribute to the highly interconnected granule cell hubs that have been proposed as crucial to development of a hyperexcitable, potentially seizure-prone circuit.

Keywords

hippocampus; mossy fiber; basal dendrite; neurogenesis; aberrant migration

Temporal lobe epilepsy is the most common form of epilepsy in the adult population (Engel, 2001). Although temporal lobe epilepsy can arise from numerous causes, most cases are believed to develop after a lesion of the brain. In lesional temporal lobe epilepsy, both in humans and in animal models, granule cells of the dentate gyrus become interconnected through the growth of mossy fibers (reviews: Nadler, 2003, 2009). Seizures also increase the rate of granule cell replication, and some of these newly generated neurons migrate to ectopic locations, most notably the dentate hilus (Parent et al., 1997, 2006; Scharfman et al., 2000; Jiao and Nadler, 2007; Jessberger et al., 2007b; Walter et al., 2007; Kron et al., 2010).

*CORRESPONDENCE TO: J. Victor Nadler, Department of Pharmacology and Cancer Biology, Box 3813, Duke University Medical Center, Durham, NC 27710. nadle002@acpub.duke.edu.

Present address for Ren-Zhi Zhan: Institute of Physiology, Shandong University School of Medicine, 44 Wenhua Xi Road, Jinan, Shandong, P.R. China.

Finally, many of the newly generated granule cells, whether normotopic (Spigelman et al., 1998; Buckmaster and Dudek, 1999; Ribak et al., 2000; Walter et al., 2007; Kron et al., 2010) or ectopic (Scharfman et al., 2000, 2003; Dashtipour et al., 2001; Kron et al., 2010), retain a hilar basal dendrite, which provides a novel surface for innervation by mossy fibers (Ribak et al., 2000). Formation of this unique reverberating network is associated with a reduced threshold for granule cell synchronization (Tauck and Nadler, 1985; Masukawa et al., 1992; Patrylo and Dudek, 1998; Hardison et al., 2000; Okazaki and Nadler, 2001; Gabriel et al., 2004). Computational models indicate that the development of even modest recurrent excitatory circuitry in the dentate gyrus should be sufficient to synchronize granule cell discharge (Santhakumar et al., 2005; Dyhrfield-Johnsen et al., 2007). Granule cell synchronization may contribute to a progressive increase in the frequency and duration of spontaneous seizures (Gorter et al., 2001; Zhang et al., 2002), because in nonepileptic animals dentate granule cells resist the propagation of seizures from the entorhinal cortex to the hippocampus (Collins et al., 1983; Stringer et al., 1989; Lothman et al., 1992).

An estimated 21-25% of dentate granule cells born after pilocarpine-induced status epilepticus migrate aberrantly into the dentate hilus (Walter et al., 2007; Kron et al., 2010). Hilar ectopic granule cells (HEGCs) account for ≈1% of the total granule cell population in these animals. Only a few granule cells are located in the hilus normally (Marti-Subirana et al., 1986; Scharfman et al., 2003; Jiao and Nadler, 2007). HEGCs survive for months at least after status epilepticus (McCloskey et al., 2006; Jessberger et al., 2007b; Jiao and Nadler, 2007) and some percentage of newborn granule cells continue to migrate aberrantly even after the replication rate normalizes (Bonde et al., 2006). Thus, the fraction of granule cells that is ectopically located may increase with time after the initial insult. Granule cell neurogenesis may be enhanced in humans with temporal lobe epilepsy as well. Some findings support the hypothesis that seizures induce neurogenesis in young patients (Siebzehnrubl and Blümcke, 2008) and HEGCs have been found in tissue resected from persons with epilepsy (Houser et al., 1992; Parent et al., 2006).

The increased frequency and duration of spontaneous seizures with time after status epilepticus in rats with neuronal death and mossy fiber sprouting (the “progression of seizures”) has been linked to enhanced granule cell neurogenesis (Jung et al., 2004, 2006). It is uncertain whether seizure progression relates to postseizure-generated granule cells that migrate normally, aberrantly, or both. Many HEGCs burst spontaneously (Scharfman et al., 2000; Zhan and Nadler, 2009a) and they are active during experimental limbic seizures (Scharfman et al., 2002). In addition, the nucleus of HEGCs is indented, unlike that of normal granule cells, consistent with a high rate of activity (Dashtipour et al., 2001). Finally, HEGCs receive an unusually high ratio of excitatory to inhibitory innervation (Zhan and Nadler, 2010). These findings suggest that HEGCs contribute to circuit hyperexcitability. Other findings suggest that postseizure-generated granule cells which migrate normally into the granule cell body layer are less excitable than preexisting granule cells (Jakubs et al., 2006). It follows therefore that the postseizure-generated granule cells associated with seizure progression are probably HEGCs. HEGCs are synaptically connected in a way that would be expected to promote seizures: they receive innervation from the entorhinal cortex, interconnect with the normotopic granule cell population, and project to CA3 pyramidal cells (Parent et al., 1997; Scharfman et al., 2000, 2003). The present study investigated the degree to which HEGCs integrate into the granule cell network of epileptic brain. We also compared the morphologies of bursting and nonbursting HEGCs.

MATERIALS AND METHODS

Pilocarpine administration

Male Sprague-Dawley rats (150-200 g; Zivic Laboratories, Pittsburgh, PA, or Charles River, Raleigh, NC) received a single injection of pilocarpine hydrochloride (340-380 mg/kg, intraperitoneally [i.p.]) 30 minutes after pretreatment with scopolamine methyl bromide and terbutaline hemisulfate (both 2 mg/kg, i.p.). Status epilepticus, defined as a continuous limbic motor seizure of stage 2 or higher (Racine, 1972), was allowed to self-terminate after 6-8 hours. Rats that experience pilocarpine-induced status epilepticus under these conditions develop extensive and consistent hilar lesions followed by consistently robust mossy fiber sprouting, the accumulation of HEGCs, and spontaneous seizures (Sloviter et al., 2003; Jiao and Nadler, 2007). Some rats exhibited only a few brief behavioral seizures, but not status epilepticus. They were used as controls to account for any possible action of pilocarpine not mediated by status epilepticus. Histological tests revealed no evidence of neuronal degeneration or mossy fiber sprouting in these animals (Okazaki et al., 1999). A total of 108 rats that had experienced pilocarpine-induced status epilepticus and 30 control rats were used in this study. All experiments were performed in accordance with the National Institutes of Health *Guide for the Care and Use of Laboratory Animals* and were approved in advance by the Duke University Institutional Animal Care and Use Committee.

Visualization of granule cell morphology

Transverse brain slices of 420-μm thickness that included the caudal hippocampus were prepared 10-40 weeks after pilocarpine administration. A slice was transferred to a submersion-type recording chamber and superfused at ≈3 mL/min and 22-24°C or 34-35°C with artificial cerebrospinal fluid that contained 122 mM NaCl, 25 mM $NaHCO_3$, 3.1 mM KCl, 1.8 mM $CaCl_2$, 1.2 mM $MgSO_4$, 0.4 mM KH_2PO_4, and 10 mM D-glucose, equilibrated with 95% O_2 / 5% CO_2. Dentate granule cells were filled with biocytin (Sigma, St. Louis, MO) during whole-cell patch clamp recordings or when the membrane patch was broken after perforated patch recordings. Recordings were made with several different internal solutions, all of which contained 0.8% or 1% (w/v) biocytin. Cells were visualized with a Nikon Eclipse E600FN microscope equipped with far infrared-differential interference contrast optics, a CCD camera, and a 40× water-immersion objective. Normotopic granule cells were studied in slices prepared from both control rats and rats that had experienced status epilepticus. The normotopic dentate granule cells selected for recording were located in the granule cell body layer at the apex of the granule cell arch or in the suprapyramidal blade close to the apex. HEGCs were studied only in rats that had experienced status epilepticus. Criteria for selecting HEGCs were 1) soma located within the hilus and of a size and shape indistinguishable from granule cells in the cell body layer and 2) no more than three dendrites emerged from the soma. Numerous cells scattered throughout the dentate hilus met these criteria, comprising an average of 62% of the total hilar neuron population (Jiao and Nadler, 2007). HEGCs filled with biocytin were located in all parts of the hilus. However, few cells located deep within the hilus, adjacent to the end of area CA3c, were studied, because it became difficult to visualize cells in this region after status epilepticus. Cell identity was confirmed by intracellular dialysis with biocytin and subsequent visualization of cellular morphology. Results obtained from putative HEGCs were included in this study only if cellular morphology appeared identical to previous descriptions of HEGCs (Scharfman et al., 2000, 2003; Dashtipour et al., 2001): small (8-12 μm diameter) soma located within the dentate hilus, 1-2 apical dendrite(s) penetrating into or directed toward the dentate molecular layer, and axons with extensive branches in the hilus, some having giant boutons. If the axon extended to area CA3 within the slice, giant boutons were observed in that region as well.

In some experiments on HEGCs we determined whether the cell was capable of bursting. A cellular burst was defined as two or more action potentials superimposed on a single depolarizing wave. Each bursting HEGC whose morphology was analyzed in this study was identified in at least one of the following three ways (Fig. 1). 1) Perforated patch recordings were made in current clamp mode. The internal solution contained 120 mM potassium gluconate, 10 mM KCl, 10 mM HEPES, 0.1 mM EGTA, 1 mM $MgCl_2$, 40 μg/mL gramicidin, and 0.8% (w/v) biocytin, pH 7.3, and 289 mOsm. Spontaneous bursting was recorded at the resting membrane potential after the series resistance had dropped below 20 MΩ. At the end of the experiment the membrane patch was broken and the cell filled with biocytin. 2) Whole-cell patch clamp recordings were made in current clamp mode. The recording was examined upon break-in for the presence of spontaneous cellular bursts at the resting membrane potential. 3) Whole-cell current clamp recordings were made with either a potassium methylsulfate (Zhan and Nadler, 2009a) or potassium gluconate (125 mM potassium gluconate, 7 mM KCl, 0.1 mM EGTA, 10 mM HEPES, 2 mM Tris ATP, 5 mM creatine phosphate, 0.3 mM Tris GTP, 20 U/mL creatine phosphokinase, and 1% (w/v) biocytin, pH 7.25-7.30, and 294-297 mOsm) -based internal solution. A series of current injections from −0.5 to +1.9 nA was made in 0.1-nA increments for 1 second each and the traces were examined for the presence of evoked bursts. HEGCs were considered to be bursting cells if they fired a burst of action potentials as their minimal response to membrane depolarization. The mean burst threshold was −55 mV. HEGCs were considered to be nonbursting only when no spontaneous or depolarization-evoked cellular bursts were detected in the second and third tests. Nonbursting HEGCs were not identified from perforated patch recordings.

After recording, the electrode tip was withdrawn slowly and the slice was fixed with 5% (w/v) paraformaldehyde in 0.1 M sodium phosphate/0.8% (w/v) NaCl (PBS). After fixation at 4 ° overnight, the slice was cut into 60-μm-thick sections with a vibratome. Sections were incubated in 30% (v/v) methanol/2% (v/v) H_2O_2 for 90 minutes to inactivate endogenous peroxidases. After washing with PBS, sections were incubated at 4 ° overnight in an avidin-horseradish peroxidase solution (Vectastain Elite ABC Kit; Vector Laboratories, Burlingame, CA) that contained 0.3% (v/v) Triton X-100. After washing again with PBS, color was developed with diaminobenzidine/H_2O_2 for 6 minutes and intensified with nickel ammonium sulfate according to the Vector protocol.

Morphological analysis

Visualized granule cells were selected for qualitative analysis if at least their cell body and dendritic tree were darkly stained and if only one cell had been labeled with biocytin in that slice. Cell morphology was reconstructed from serial sections with use of Neurolucida (MBF Bioscience, Williston, VT). Traces of the cell body and dendrites were made while viewing the biocytin-labeled cell through a 40× objective. Neurolucida was also used to measure dendritic length and branching. No correction was applied for shrinkage. Thus, our values underestimate the true dendritic length. However, they remain useful for between-group comparisons. Percentage incidences of a hilar basal dendrite, recurrent mossy fiber in the dentate molecular layer, and mossy fiber in stratum lucidum of area CA3 were compared with a χ-square test. Dendritic lengths and branching (total number of branch points obtained from Scholl analysis) were not normally distributed. The results are therefore expressed as median and range, and between-group comparisons were made with either the Mann-Whitney rank sum test (two groups) or the Kruskal-Wallis one-way analysis of variance (ANOVA) on ranks (more than two groups). Between-group differences in branching within different segments of the dendritic tree were assessed with a two-way ANOVA (granule cell group × dendritic segment), followed by breakdown of the ANOVA and Newman-Keuls test.

Digitized images were modified only to improve brightness, contrast, and sharpness with use of PaintShop Photo Pro X3 (Corel, Mountain View, CA). Identical changes were applied to all the images in a given composite figure.

Membrane properties

During whole cell recordings, resting V_m was determined in current clamp mode immediately on break-in. During perforated patch recordings, resting V_m was determined in current clamp mode when the series resistance fell below 20 MΩ. Input resistance was determined from the current response to a 10-mV hyperpolarization from resting V_m applied for 200 ms. Values of resting V_m and input resistance were normally distributed. The results are therefore expressed as mean ± SEM, and between-group comparisons were made with Student's *t*-test.

RESULTS

According to our criteria, 40 normotopic dentate granule cells from control rats (CGCs), 54 normotopic granule cells from rats that had experienced pilocarpine-induced status epilepticus (GC-SEs), and 79 HEGCs were visualized sufficiently well to permit qualitative analysis of their dendritic tree. The CGCs were obtained from 30 rats, the GC-SEs from 50 rats, and the HEGCs from 64 rats. Of these cells, 17 CGCs, 20 GC-SEs, and 44 HEGCs were randomly selected for quantitative analysis. CGCs selected for quantitative analysis were obtained from 13 rats, the GC-SEs from 20 rats, and the HEGCs from 39 rats. In granule cells from all groups, nearly all the biocytin-labeled cell processes were usually present in just 4 of the 6-7 sections cut from each slice. This observation suggests that the axonal projections and dendritic tree of HEGCs, like those of normotopic granule cells, are oriented predominantly in the transverse plane, and they span about the same distance along the rostrocaudal axis of the hippocampus.

HEGCs have sparsely branched apical dendrites

Biocytin-labeled granule cells had one or two spiny apical dendrites. Apical dendrites of all the labeled CGCs and GC-SEs reached the outer edge of the molecular layer (Fig. 2). This observation suggests labeling of the entire dendritic tree, although amputation of some dendritic branches may have occurred during slice preparation in some instances. The distal third of GC-SE apical dendrites appeared somewhat more extensively branched than the distal third of CGC apical dendrites. As reported previously (Scharfman et al., 2000, 2003), HEGCs fell into two groups with respect to the termination of their apical dendrite(s): the apical dendrite(s) of 86% (68/79) extended to the outer edge of the dentate molecular layer and the single apical dendrite of the remaining 14% (11/79) was confined to the hilus. HEGCs in the latter group always had two dendrites that arose from opposite poles of the soma. The dendrite oriented toward the granule cell body layer was regarded as the apical dendrite and the dendrite oriented away from the granule cell body layer was regarded as the basal dendrite. In general, the apical dendrites of HEGCs that penetrated the molecular layer appeared less well branched than the apical dendrites of GC-SEs or CGCs.

Quantitative analyses confirmed the between-group differences in apical dendritic structure suggested by our visual observations. The total apical dendritic length and extent of branching of GC-SEs was significantly greater than that of HEGCs with dendrites in the molecular layer (Table 1; $P < 0.05$ by Dunn's test in each case). As expected, the total apical dendritic length of HEGCs with dendrites in the molecular layer was significantly greater than that of HEGCs whose dendrites were confined to the hilus ($P < 0.05$ by Mann-Whitney rank sum test). However, the difference was less than might be expected, because the extent of branching was the same. Thus, HEGCs with dendrites confined to the hilus had a more

compact apical dendritic tree, with considerably greater branching per length of dendrite. Scholl analysis revealed significantly reduced apical dendritic length and branching in HEGCs than in either GC-SEs or CGCs beginning at 50 μm from the soma (Fig. 3). Scholl analysis also confirmed that apical dendritic length and branching in the outer third of the molecular layer, the terminal zone of the lateral perforant path, was significantly greater in GC-SEs than in CGCs.

HEGCs are more likely than other granule cells to have a hilar basal dendrite

HEGCs were much more likely to have a hilar basal dendrite than GC-SEs: 62% (49/79) compared with 20% (11/54) (Fig. 4). No cell had more than one basal dendrite. The basal dendrites of both granule cell types were invested with spines. The basal dendrite of GC-SEs was either unbranched or branched once just after its origin from the soma. In contrast, the basal dendrite of HEGCs branched either close to the soma, more distally, or both. In general, the basal dendritic tree of most HEGCs appeared larger and more extensively branched than GC-SE basal dendritic trees: the basal dendritic tree of 19 of the 35 HEGCs analyzed quantitatively was larger than the largest basal dendritic tree of any quantitatively analyzed GC-SE. There was considerable overlap, however, accounting for the lack of statistically significant differences (Table 1; $P = 0.104$ for length and $P = 0.063$ for branching by Mann-Whitney rank sum test).

The hilar basal dendrite of those HEGCs having apical dendrites that traversed the dentate molecular layer contributed more to the total dendritic length than the hilar basal dendrite of GC-SEs (median of 14% [range: 1-85%] compared with median of 6% [range: 3-13%]; $P = 0.05$ by the Mann-Whitney rank sum test). As expected, the basal dendrite of those HEGCs whose dendrites were confined to the hilus contributed more to the total dendritic length than the basal dendrite of those HEGCs having apical dendrites that traversed the molecular layer (median of 50% [range: 20-60%] compared with median of 14% [range: 1-85%]; $P < 0.005$ by the Mann-Whitney rank sum test).

GC-SEs with a hilar basal dendrite are considered to have either still been differentiating at the time of status epilepticus or to have been born into the postseizure environment (Kron et al., 2010). These relatively young cells are located mainly in the portion of the cell body layer closest to the hilus, although some would have migrated farther away from the hilar border by the time we studied them (Parent et al., 1997; Shapiro and Ribak, 2005). No attempt was made to select GC-SEs at any particular depth within the cell body layer. However, of the 11 GC-SEs studied that had a hilar basal dendrite, nine (88%) were located in the inner third of the layer, that is, the portion closest to the hilus. Of all the GC-SEs studied whose soma was located in the inner third, 53% had a hilar basal dendrite. The other two GC-SEs with a hilar basal dendrite were located in the middle third of the layer, accounting for 7% of the GC-SEs studied that were located there.

Dentate granule cells in normal rodents rarely have a basal dendrite that remains within the hilus; only a few such cells have been described (Ribak et al., 2000; Thind et al., 2008). Status epilepticus markedly increases the percentage of normotopic granule cells with a hilar basal dendrite. The percentage also increases significantly, albeit to a much lesser degree, in rats that experience only several brief behavioral seizures after being treated with pilocarpine (Ribak et al., 2000). The granule cells used as controls for the present study (CGCs) were from rats that had experienced brief behavioral seizures after pilocarpine administration, but not status epilepticus. Thus, we expected some of them to have a basal dendrite. This result was indeed obtained; a short hilar basal dendrite was observed in 5 of 40 (12%) CGCs. All of them were about the same length as the shortest HEGC or GC-SE basal dendrite. Basal dendrites of CGCs were unbranched and appeared to lack spines (Fig.

4C). Two of them were analyzed quantitatively. Dendritic lengths were 52 and 61 μm, accounting for 5.1% and 2.3% of the total (apical + basal) dendritic length, respectively.

HEGCs are more likely than other granule cells to send a recurrent mossy fiber into the dentate molecular layer

Biocytin either filled the entire mossy fiber, including synaptic terminals, or failed to enter the mossy fiber at all. Mossy fiber projections of 55 HEGCs, 32 GC-SEs, and 33 CGCs were filled well enough to assess their projections to different postsynaptic targets.

Mossy fibers transmit signals from dentate granule cells to the pyramidal cells of hippocampal area CA3. Although serving as a key link in the excitatory trisynaptic circuit (layer 2 stellate cells of the entorhinal cortex → dentate granule cells → CA3 pyramidal cells → CA1 pyramidal cells) is the best-recognized function of the mossy fibers, they innervate predominantly inhibitory interneurons of the dentate hilus and area CA3 (Acsády et al., 1998). Most branches are distributed within the dentate hilus. HEGCs and GC-SEs appeared identical to CGCs in this respect. Mossy fibers of HEGCs were about as likely as mossy fibers of normotopic granule cells to project to CA3 pyramidal cells within the slice (Fig. 5). Of the HEGCs whose mossy fiber was labeled with biocytin, 89% sent a branch into stratum lucidum of area CA3, compared with 86% of similarly labeled GC-SEs and 85% of CGCs. The mossy fibers of HEGCs, like those of normotopic granule cells, had widely spaced giant boutons in stratum lucidum from which filopodia emerged. The giant boutons are presynaptic to thorny excrescences of CA3 pyramidal cells, whereas the filopodia and smaller boutons form synapses with interneurons (Acsády et al., 1998).

HEGCs were much more likely to send at least one recurrent mossy fiber into the dentate molecular layer than GC-SEs (84% compared with 38%; Fig. 6). For half the HEGCs with recurrent mossy fibers (23/46), 2-4 separate branches were observed to emerge from the hilus and enter the molecular layer. For the other HEGCs, only one such branch was visible. In 30% of HEGCs with recurrent mossy fibers, further branching was observed in the granular and molecular layers. HEGC recurrent mossy fibers were studded with relatively small boutons comparable to most of those within the hilus, turned when they reached the inner third of the molecular layer, and coursed parallel to the granule cell body layer. All branches were usually confined to the inner third of the molecular layer. In three instances, however, the recurrent mossy fiber reached the perforant path terminal zone.

The recurrent mossy fibers of GC-SEs visualized in the present study resembled those of HEGCs, as well as the biocytin-labeled recurrent mossy fibers shown in previous reports (Okazaki et al., 1995; Sutula et al., 1998; Buckmaster et al., 2002). We noted only one difference between the recurrent mossy fibers of HEGCs and GC-SEs: namely, that those emanating from GC-SEs never extended beyond the inner third of the molecular layer. GC-SEs having a recurrent mossy fiber, like those having a hilar basal dendrite, are thought to have been generated either during the postseizure period or within 5 weeks before status epilepticus (Kron et al., 2010). However, the 12 GC-SEs with a recurrent mossy fiber were less likely to be located in the inner third of the granule cell body layer than GC-SEs with a hilar basal dendrite. Only half were located in the inner third and two-thirds of those located there (4/6) also had a hilar basal dendrite. Of the other six GC-SEs with a recurrent mossy fiber, five were located in the middle third of the cell body layer and one was located in the outer third. None of these cells had a hilar basal dendrite. GC-SEs with a recurrent mossy fiber accounted for 35% of all GC-SEs studied that were located in the inner third of the layer, 17% of those located in the middle third of the layer, and 14% of those located in the outer third of the layer. When GC-SEs that also had a hilar basal dendrite were excluded from the calculations, the probability of a recorded GC-SEs having a recurrent mossy fiber was about the same at all depths of the cell body layer.

Mossy fibers of two CGCs also had a recurrent branch in the molecular layer. Unlike the recurrent mossy fibers of HEGCs and GC-SEs, the recurrent branch of control mossy fibers penetrated only a short distance beyond the granule cell body layer and did not turn to course parallel to this layer.

HEGCs that sent one or more recurrent mossy fibers into the dentate molecular layer were also likely to have a hilar basal dendrite (30/46; 65%). As noted above, only one-third (4/12) of GC-SEs with recurrent mossy fibershad a hilar basal dendrite and neither CGC did. HEGCs having a hilar basal dendrite were also likely to have a recurrent mossy fiber in the molecular layer. Considering only those cells whose mossy fiber was visualized adequately, 80% (28/35) of these HEGCs had both recurrent mossy fiber and hilar basal dendrite. Four of the seven GC-SEs with a hilar basal dendrite and an adequately labeled mossy fiber also had one or more recurrent mossy fibers, but none of three CGCs did.

Some bursting HEGCs exhibit unusual dendritic morphology

Visualization of intracellular biocytin revealed the cell morphology of 18 confirmed bursting HEGCs and eight confirmed nonbursting HEGCs. Bursting HEGCs could fire both spontaneous and depolarization-evoked bursts or only depolarization-evoked bursts, as reported previously (Zhan and Nadler, 2009a). Of the 18 biocytin-labeled bursting HEGCs, 14 were found to be bursting spontaneously. In the four HEGCs that did not burst spontaneously, step depolarization of the cell by current injection evoked a cellular burst as their minimal response. Six HEGCs that fired bursts spontaneously were tested with step depolarizations to determine whether that stimulus could evoke a cellular burst. Depolarization induced burst firing in all of these cells. A similar result was obtained in six additional spontaneously bursting HEGCs not included in the present study. Depolarization above burst threshold (−55 mV) evoked a train of action potentials in which the first response was always a burst. Addition of glutamate receptor antagonists (10 μM 2,3-dihydroxy-6-nitro-7-sulfamyl-benzo(F)quinoxaline-2,3-dione [NBQX] and 50 μM 2-amino-5-phosphonopentanoate [D-AP5]) to the superfusion medium did not affect depolarization-evoked bursting (n = 2). The rate of spontaneous bursting was greatest in HEGCs with the lowest resting membrane potentials (Zhan and Nadler, 2009a). In addition, spontaneous bursting could be terminated by injecting sufficient hyperpolarizing current. These results indicate that many HEGCs possess an intrinsic burst mechanism.

Bursting HEGCs had a significantly smaller and less branched dendritic tree than nonbursting HEGCs (Table 2). In part, this difference could be explained by the greater propensity for the dendrites of bursting HEGCs to remain confined within the hilus. The apical dendrite(s) of 20 of the 26 reconstructed HEGCs traversed the granule cell body layer and reached the outer molecular layer. Dendrites of the other six were confined to the dentate hilus. Of the six HEGCs whose dendrites were confined to the hilus, five were bursting cells. However, even when the statistical analysis included only those HEGCs whose apical dendrite(s) penetrated the molecular layer, the total dendritic length and branching of bursting HEGCs was still significantly less than that of nonbursting HEGCs. These between-group differences were accounted for entirely by bursting HEGCs having a less extensive and less branched apical dendritic tree (Table 3). The apical dendrites of nonbursting HEGCs resembled those of GC-SEs (cf. Tables 1, 3). In contrast, bursting and nonbursting HEGCs were about equally likely to have a hilar basal dendrite (bursting: 11/18, 61%; nonbursting: 5/8, 62%), and there was no apparent difference in basal dendritic length or extent of branching.

Part of the apical dendrite of all HEGCs resides within the hilus. The intrahilar portion of the apical dendrite may be innervated differently from the portion in the molecular layer, perhaps similarly to the basal dendrite. If the proportion of the dendritic tree located within

the hilus differed for bursting and nonbursting cells, the corresponding differences in innervation might contribute to bursting. The percentage of the apical and total dendritic length in the hilus indeed tended to be greater in bursting than in nonbursting HEGCs, but these differences were not statistically significant (Table 2). Much, if not all, of this apparent difference could be ascribed to the greater proportion of bursting HEGCs whose dendrites were confined entirely to the hilus.

Four of the bursting HEGCs whose dendrites remained within the hilus and two whose dendrites traversed the molecular layer exhibited dendritic features similar to those of immature granule cells (Jones et al., 2003; Ambrogini et al., 2004; Zhao et al., 2006). Abnormal findings included unusually short dendritic length, numerous varicosities, and few or no mature spines (Fig. 7). Possibly, the rarity of mature spines might reflect insufficient biocytin labeling, rather than a true morphologic abnormality. It seems unlikely, however, that biocytin labeling was sufficient to reveal mature dendritic spines in all the other recorded cells, yet not in this subpopulation of bursting HEGCs. The total dendritic lengths of four bursting HEGCs, three with dendrites confined entirely to the hilus and one whose apical dendrite penetrated into the molecular layer, were <400 μm. Although the resting membrane potentials and input resistances of bursting HEGCs as a group did not differ significantly from those of nonbursting HEGCs (Table 2), the input resistances of these four cells were above average (356-667 MΩ). High input resistance is also characteristic of immature dentate granule cells (Liu et al., 1996; Ambrogini et al., 2004; Schmidt-Hieber et al., 2004; Overstreet-Wadiche and Westbrook, 2006). No biocytin-labeled nonbursting HEGC exhibited an unusually short total dendritic length, abnormal dendritic morphology, or unusually high input resistance. Thus, the dendrites of 39% (7/18) of bursting HEGCs were either confined to the hilus, appeared morphologically immature, or both, compared with 12% (1/8) of the nonbursting HEGCs.

In other respects, there were no consistent differences between bursting and nonbursting HEGCs. The somata of both groups could be located anywhere within the hilus. Those bursting and nonbursting HEGCs whose axons were visualized with biocytin were also about equally likely to send a recurrent mossy fiber branch into the dentate molecular layer (bursting: 7/10, 70%; nonbursting: 4/6, 67%).

DISCUSSION

The most important finding of this study is that the axons and dendrites of HEGCs distribute in a manner that suggests these cells integrate more tightly into the dentate granule cell network of epileptic brain than GC-SEs. They are more than three times as likely to have a hilar basal dendrite as normotopic granule cells. Granule cell basal dendrites expand the dendritic surface available for innervation by mossy fibers (Ribak et al., 2000). HEGCs are as likely as normotopic granule cells to project a mossy fiber with giant boutons to stratum lucidum of area CA3, but are more than twice as likely to send one or more recurrent mossy fibers into the dentate molecular layer. The postsynaptic targets of mossy fibers have been identified with certainty only for mossy fibers of normotopic granule cells. Mossy fibers of HEGCs are morphologically similar to those of GC-SEs and project to the same locations. Although further studies are required to confirm that the mossy fibers of ectopic and normotopic granule cells have the same postsynaptic targets, this Discussion assumes that they do. Based on this assumption, we conclude that HEGCs, like normotopic dentate granule cells, innervate CA3 pyramidal cells, but are more than twice as likely as GC-SEs to innervate other granule cells. These cells are much more excitable than normotopic granule cells. About half of them burst spontaneously and/or in response to a step depolarization (Zhan and Nadler, 2009a). Bursting HEGCs appear as likely as nonbursting HEGCs to integrate into dentate gyrus circuitry. Furthermore, HEGCs receive a much higher ratio of

excitatory to inhibitory innervation than normotopic granule cells (Zhan and Nadler, 2010). Our findings indicate that, once engaged in epileptiform activity, GC-SEs have many paths along which to transmit their synchronized activity to HEGCs. Conversely, HEGCs have many paths along which to transmit their spontaneous and evoked hyperactivity to both GC-SEs and CA3 pyramidal cells. These relationships support the hypothesis that HEGCs account for the negative effects of postseizure neurogenesis, including an increased frequency and duration of spontaneous seizures (Jung et al., 2004, 2006) and disruption of hippocampus-dependent learning (Jessberger et al., 2007a; Pekcec et al., 2008). Consistent with this hypothesis, modeling studies indicate that a small population of highly interconnected granule cell hubs should greatly increase activity in the granule cell network, resulting in a hyperexcitable, potentially seizureprone circuit (Morgan and Soltesz, 2008). The axonal and dendritic morphology of HEGCs suggests that they contribute to these hubs.

Seizure-related changes in granule cell morphology

Dentate granule cells normally have a hilar basal dendrite during their early development, but it either retracts or evolves into an apical dendrite as the cell migrates into the cell body layer and differentiates (Shapiro and Ribak, 2005). Most HEGCs and some GC-SEs retain a hilar basal dendrite (Shapiro and Ribak, 2005; Jessberger et al., 2007b; Walter et al., 2007; Kron et al., 2010). Kron et al. (2010) reported that only those granule cells that were born after or within 5 weeks before status epilepticus retain a hilar basal dendrite or send recurrent mossy fibers into the dentate molecular layer. The localization of GC-SEs with a hilar basal dendrite in the present study supports this hypothesis; 88% of them were located close to the hilar border of the granule cell body layer, which coincides with the location of the youngest cells. However, GC-SEs with a recurrent mossy fiber were found at all depths of the granule cell body layer, even close to the molecular layer. This finding could be interpreted to suggest that the mossy fibers of some mature dentate granule cells also develop a recurrent branch after status epilepticus. Another possibility is that those newly generated GC-SEs that migrate farthest from their birthplace in the subgranular zone tend to retain their recurrent mossy fiber, but to either lose their basal dendrite or transform it into a second apical dendrite.

Populations of HEGCs and GC-SEs having a hilar basal dendrite overlap with the populations having a recurrent mossy fiber, but they are not identical. Granule cells of both types may have either or both processes. HEGCs are more likely to have both than GC-SEs. Because recurrent mossy fiber sprouting and retention of a hilar basal dendrite can occur in different cells, these morphological changes must have different underlying mechanisms. Pilocarpine-induced status epilepticus destroys the great majority of hilar mossy cells (Buckmaster and Jongen-Rêlo, 1999; Sloviter et al., 2003; Jiao and Nadler, 2007), an average of 95% when performed by the method used in the present study (Jiao and Nadler, 2007). The associational-commissural axons of hilar mossy cells provide excitatory innervation to the proximal third of the granule cell apical dendrite (Ribak et al., 1985). The extent of recurrent mossy fiber sprouting after status epilepticus is directly proportional to the loss of GluR2-immunoreactive hilar mossy cells (Jiao and Nadler, 2007). Therefore, the resultant loss of associational-commissural synapses may trigger formation of these axon collaterals. Retention of a hilar basal dendrite must depend largely on some other consequence of status epilepticus.

Excitatory synaptic innervation of HEGCs

Electron microscopic (Dashtipour et al., 2001; Pierce et al., 2005) and electrophysiological studies (Zhan and Nadler, 2010) demonstrated the innervation of HEGCs by mossy fibers. The proximal apical dendrites of HEGCs are more densely innervated by mossy fibers than the proximal apical dendrites of GC-SEs in the same animals (Pierce et al., 2005). Mossy

fiber synapses are also much more abundant on the soma of HEGCs than of GC-SEs (Dashtipour et al., 2001). Finally, mossy fibers probably innervate the hilar basal dendrite of HEGCs. The hilar basal dendrite of GC-SEs receives predominantly excitatory innervation (Thind et al., 2008), at least some of which is derived from mossy fibers (Ribak et al., 2000). HEGCs are much more likely to have a hilar basal dendrite than GC-SEs and the basal dendritic tree of HEGCs, on average, offers a larger surface for synaptogenesis. Assuming the hilar basal dendrite of HEGCs is innervated similarly to that of GC-SEs, then HEGCs probably receive considerably more mossy fiber innervation than GC-SEs. HEGCs whose apical dendrite(s) penetrates the molecular layer also receive monosynaptic innervation from the entorhinal cortex by way of the perforant path (Scharfman et al., 2003). HEGCs may, however, receive less perforant path innervation than GC-SEs. HEGC apical dendrites that penetrate the molecular layer have less dendritic surface available for synapse formation with perforant path fibers. HEGCs whose dendrites are confined to the hilus probably receive no direct innervation from the perforant path (Scharfman et al., 2003).

We recorded miniature excitatory postsynaptic currents (mEPSCs) from HEGCs about twice as frequently as from GC-SEs or CGCs (Zhan and Nadler, 2010). Morphological analysis of these cells suggests that differences in mEPSC frequency cannot be explained by differences in the length of dendrite available for synaptogenesis. Although the total length and branching of HEGC apical dendrites that extend into the dentate molecular layer are less, on average, than those of GC-SE apical dendrites, the relatively large basal dendritic tree makes up for this deficit. Thus, there was no significant between-group difference when the lengths of apical and basal dendrites were combined. The high frequency of mEPSCs in HEGCs may be explained by a greater number of excitatory synapses per dendritic length or by a higher probability of action potential-independent glutamate release.

Recurrent mossy fibers of HEGCs

When associational-commissural connections degenerate or fail to form due to the seizure-induced death of hilar mossy cells, granule cell mossy fibers sprout collaterals that establish synapses on the denervated (GC-SEs) or noninnervated (HEGCs) dendritic region of other granule cells, thus replacing the synapses that had been lost. Recurrent mossy fibers that originate from GC-SEs innervate primarily granule cells; 95% of their synapses are made with granule cells and only 5% with inhibitory interneurons (Buckmaster et al., 2002). If the synapses made by the recurrent mossy fibers of HEGCs are distributed similarly, our finding that 84% of the biocytin-labeled HEGCs sent at least one axonal branch into the dentate molecular layer suggests that a significant percentage of the recurrent mossy fiber innervation received by dentate granule cells in epileptic brain arises from these cells. Moreover, some of these recurrent mossy fibers extended beyond the inner third of the molecular layer to reach the perforant path terminal zone. We previously described recurrent mossy fibers that penetrate the perforant path terminal zone (Okazaki et al., 1995) and now conclude that at least some of them arise from HEGCs.

Our assessment of mossy fiber projections to area CA3 suggests that our count of HEGCs with a recurrent mossy fiber underestimated their actual incidence, and thus their influence over activity in the granule cell network. Every dentate granule cell is believed to send a mossy fiber branch through stratum lucidum of area CA3. In the present study, we confirmed that 85-89% of the biocytin-labeled cells in each granule cell population had such a branch. In those cases where a mossy fiber branch did not reach area CA3 within the slice, it is likely that the branch was cut at some point within the hilus during slice preparation. If a similar percentage of recurrent mossy fibers were cut before they reached the dentate molecular layer, we may conclude that all or nearly all HEGCs have a recurrent mossy fiber. This conclusion is consistent with findings that mossy fiber sprouting is confined to those granule cells that were born either after or within 5 weeks before status epilepticus (Kron et

al., 2010) and that only granule cells born into the postseizure environment migrate aberrantly into the dentate hilus (Walter et al., 2007; Kron et al., 2010).

Does HEGC bursting reflect cellular immaturity?

Cellular bursting can be driven in three ways: by intrinsic mechanisms alone (Sanabria et al., 2001), by excitatory synaptic activity alone (i.e., a "giant" excitatory postsynaptic potential [EPSP]; Perrault and Avoli, 1991; Funahashi and Stewart, 1997), or by synaptic excitation that provides the depolarization required to activate an intrinsic burst mechanism. All HEGCs that burst spontaneously also fired a burst of action potentials as their minimal response to injection of depolarizing current. In addition, some HEGCs that did not exhibit spontaneous bursting fired depolarization-evoked cellular bursts. Further testing established that an intrinsic burst mechanism underlies depolarization-evoked bursts in these cells. Preliminary results suggest that the depolarization-evoked bursts and probably some spontaneous bursts require the activation of low-threshold calcium current (Zhan and Nadler, 2009b). Thus, HEGCs are not simply passive followers of bursting initiated in other neurons, as was suggested initially (Scharfman et al., 2000). However, synaptic excitation probably contributes to spontaneous bursting as well. We reported previously that spontaneous bursting could be recorded from HEGCs having a resting V_m as high as −77 mV, well above the threshold for intrinsic bursts (Zhan and Nadler, 2009a). In these instances, synaptically induced depolarization is presumably required to activate low-threshold calcium current and thus bursting. In addition, spontaneous excitatory synaptic events are larger and/or occur more frequently in HEGCs than in other granule cells (Zhan and Nadler, 2010). The coincidence of several such events may trigger a cellular burst through formation of a giant EPSP.

Several lines of evidence suggest that bursting HEGCs are less mature developmentally, and therefore possibly younger, than nonbursting HEGCs. 1) The apical dendritic tree of bursting HEGCs is less well-developed than that of nonbursting HEGCs. 2) The dendritic morphology of a minority of bursting HEGCs exhibits features typical of immature dentate granule cells, including an unusually short dendritic length, little branching, numerous varicosities, and few or no mature spines. 3) Bursting HEGCs of this type also have a relatively high input resistance. 4) Depolarization evokes a low-threshold calcium current an order of magnitude larger in bursting HEGCs than in nonbursting HEGCs or normotopic granule cells (Zhan and Nadler, 2009b). Immature dentate granule cells also express a large low-threshold calcium current (Schmidt-Hieber et al., 2004) that diminishes during cellular differentiation. Those HEGCs having intrinsic burst capability may therefore have been generated more recently on average than nonbursting HEGCs and were still developmentally immature when recorded. Intrinsic bursting might be a property of relatively young HEGCs that is lost during further cell differentiation. Both bursting and nonbursting HEGCs were recorded at all times after status epilepticus between 10 and 40 weeks. Because HEGCs continue to be produced for months at least after status epilepticus (Bonde et al., 2006), we could not know the age of any specific recorded cell. Even 40 weeks after status epilepticus, some HEGCs are quite young. Thus, the hypothesized transition from a bursting to a nonbursting phenotype could not have been observed in the present study. Resolution of this issue will require examination of HEGCs that were labeled permanently at birth (Jessberger et al., 2007b; Walter et al., 2007; Kron et al., 2010).

Composition and apical dendritic structure of GC-SEs

Our findings also indicate significant changes in the composition and apical dendritic structure of normotopic dentate granule cells after status epilepticus. Of the GC-SEs studied, 38% had a recurrent mossy fiber that penetrated the dentate molecular layer and coursed through its inner third. In a few other instances, the recurrent mossy fiber may have been cut

during slice preparation at a site proximal to molecular layer entry. If having a recurrent mossy fiber marks those granule cells that were still differentiating at the time of status epilepticus or that were born into the postseizure environment (Kron et al., 2010), then nearly half the GC-SEs we studied fell into one or the other of these classes. That would imply either a rather dramatic expansion of the granule cell population after status epilepticus or a similarly dramatic turnover in the granule cell population, older cells being replaced by younger cells. It should be noted that we studied only those normotopic granule cells located at or close to the apex of the granule cell arch in the caudal dentate gyrus. Thus, we cannot exclude the possibility that seizure-related expansion or turnover of the granule cell population is confined to this location rather than occurring throughout the dentate gyrus. Further studies are needed to assess these possibilities. It should be noted as well that we studied granule cells that were dialyzed intracellularly with biocytin during or after patch clamp recording. Although unlikely, it is possible that we inadvertently studied younger cells out of proportion to their incidence in the population because it was easier to make a gigaohm seal on younger cells. This possibility also requires further investigation.

In addition, Scholl analysis revealed greater length and branching of the distal apical dendrites of GC-SEs than of CGCs. Pathways that project to the outer part of the dentate molecular layer undergo structural and functional reorganization after status epilepticus. Functional changes in perforant path synapses include increased glutamate release probability (Scimeni et al., 2006), reduced regulation of glutamate release by feedback activation of presynaptic mGluR7 (Bough et al., 2004) or mGluR8 (Kral et al., 2003) receptors, and prolonged NMDA receptor-mediated EPSCs (Scimeni et al., 2006). There is also a transient loss of perforant path synapses followed by their reacquisition (Nadler et al., 1980; Thind et al., 2010). Most HIPP cells, one of the two major sources of inhibitory innervation to the distal apical dendrites of dentate granule cells (Freund and Buzsáki, 1996), degenerate after experimental status epilepticus (Buckmaster and Jongen-Rêlo, 1999). Loss of these neurons leads to a commensurate loss of inhibitory synapses in the outer molecular layer. However, HIPP cells that survive status epilepticus sprout axon collaterals (Zhang et al., 2009), which may restore synaptic inhibition to that region (Thind et al., 2010). Our results suggest that these structural and functional changes in pathways that project to the outer molecular layer are matched by the growth of granule cell dendrites in the same region.

Acknowledgments

We thank Y. Jiao, X. Yuan, and D.A. Evenson for technical assistance and K. Gorham for clerical help.

Grant sponsor: National Institutes of Health; Grant numbers: NS-38108 and NS-61849.

LITERATURE CITED

Acsády L, Kamondi A, Sik A, Freund T, Buzsáki G. GABAergic cells are the major postsynaptic targets of mossy fibers in the rat hippocampus. J Neurosci. 1998; 18:3386–3403. [PubMed: 9547246]

Ambrogini P, Lattanzi D, Ciuffoli S, Agostini D, Bertini L, Stocchi V, Santi S, Cuppini R. Morpho-functional characterization of neuronal cells at different stages of maturation in granule cell layer of adult dentate gyrus. Brain Res. 2004; 1017:21–31. [PubMed: 15261095]

Bonde S, Ekdahl CT, Lindvall O. Long-term neuronal replacement in adult rat hippocampus after status epilepticus despite chronic inflammation. Eur J Neurosci. 2006; 23:965–974. [PubMed: 16519661]

Bough KJ, Mott DD, Dingledine RJ. Medial perforant path inhibition mediated by mGluR7 is reduced after status epilepticus. J Neurophysiol. 2004; 92:1549–1557. [PubMed: 15152022]

Buckmaster PS, Dudek FE. In vivo intracellular analysis of granule cell axon reorganization in epileptic rats. J Neurophysiol. 1999; 81:712–721. [PubMed: 10036272]

Buckmaster PS, Jongen-Rêlo AL. Highly specific neuron loss preserves lateral inhibitory circuits in the dentate gyrus of kainate-induced epileptic rats. J Neurosci. 1999; 19:9519–9529. [PubMed: 10531454]

Buckmaster PS, Zhang GF, Yamawaki R. Axon sprouting in a model of temporal lobe epilepsy creates a predominantly excitatory feedback circuit. J Neurosci. 2002; 22:6650–6658. [PubMed: 12151544]

Collins RC, Tearse RG, Lothman EW. Functional anatomy of limbic seizures: focal discharges from medial entorhinal cortex in rat. Brain Res. 1983; 280:25–40. [PubMed: 6652478]

Dashtipour K, Tran PH, Okazaki MM, Nadler JV, Ribak CE. Ultrastructural features and synaptic connections of hilar ectopic granule cells in the rat dentate gyrus are different from those of granule cells in the granule cell layer. Brain Res. 2001; 890:261–271. [PubMed: 11164792]

Dyhrfield-Johnsen J, Santhakumar V, Morgan RJ, Huerta R, Tsimring L, Soltesz I. Topological determinants of epileptogenesis in large-scale structural and functional models of the dentate gyrus derived from experimental data. J Neurophysiol. 2007; 97:1566–1587. [PubMed: 17093119]

Engel J. Mesial temporal lobe epilepsy: what have we learned? Neuroscientist. 2001; 7:340–352. [PubMed: 11488399]

Funahashi M, Stewart M. Presubicular and parasubicular cortical neurons of the rat: functional separation of deep and superficial neurons in vitro. J Physiol. 1997; 501:387–403. [PubMed: 9192310]

Gabriel S, Njunting M, Pomper JK, Merschhemke M, Sanabria ERG, Eilers AQ, Kivi A, Zeller M, Meencke H-J, Cavalheiro EA, Heinemann U, Lehmann T-N. Stimulus and potassium-induced epileptiform activity in the human dentate gyrus from patients with and without hippocampal sclerosis. J Neurosci. 2004; 24:10416–10430. [PubMed: 15548657]

Gorter JA, van Vliet EA, Aronica E, Lopes da Silva FH. Progression of spontaneous seizures after status epilepticus is associated with mossy fibre sprouting and extensive bilateral loss of hilar parvalbumin and somatostatin-immunoreactive neurons. Eur J Neurosci. 2001; 13:657–669. [PubMed: 11207801]

Hardison JL, Okazaki MM, Nadler JV. Modest increase in extracellular potassium unmasks effect of recurrent mossy fiber growth. J Neurophysiol. 2000; 84:2380–2389. [PubMed: 11067980]

Houser CR, Swartz BE, Walsh GO, Delgado-Escueta AV. Granule cell disorganization in the dentate gyrus: possible alterations of neuronal migration in human temporal lobe epilepsy. Epilepsy Res Suppl. 1992; 9:41–48. [PubMed: 1285913]

Jakubs K, Nanobashvili A, Bonde S, Ekdahl CT, Kokaia Z, Kokaia M, Lindvall O. Environment matters: synaptic properties of neurons born in the epileptic adult brain develop to reduce excitability. Neuron. 2006; 52:1047–1059. [PubMed: 17178407]

Jessberger S, Nakashima K, Clemenson GD, Mejia E, Mathews E, Ure K, Ogawa S, Sinton CM, Gage FH, Hsieh J. Epigenetic modulation of seizure-induced neurogenesis and cognitive decline. J Neurosci. 2007a; 27:5967–5975. [PubMed: 17537967]

Jessberger S, Zhao C, Toni N, Clemenson GD, Li Y, Gage FH. Seizure-associated, aberrant neurogenesis in adult rats characterized with retrovirus-mediated cell labeling. J Neurosci. 2007b; 27:9400–9407. [PubMed: 17728453]

Jiao Y, Nadler JV. Stereological analysis of GluR2-immunoreactive hilar neurons in the pilocarpine model of temporal lobe epilepsy: correlation of cell loss with mossy fiber sprouting. Exp Neurol. 2007; 205:569–582. [PubMed: 17475251]

Jones SP, Rahimi O, O'Boyle MP, Diaz DL, Claiborne BJ. Maturation of granule cell dendrites after mossy fiber arrival in hippocampal field CA3. Hippocampus. 2003; 13:413–427. [PubMed: 12722981]

Jung K-H, Chu K, Kim M, Jeong S-W, Song Y-M, Lee S-T, Kim J-Y, Lee SK, Roh J-K. Continuous cytosine-b-D-arabinofuranoside infusion reduces ectopic granule cells in adult rat hippocampus with attenuation of spontaneous recurrent seizures following pilocarpine-induced status epilepticus. Eur J Neurosci. 2004; 19:3219–3226. [PubMed: 15217378]

Jung K-H, Chu K, Lee S-T, Kim J, Sinn D-I, Kim J-M, Park D-K, Lee J-J, Kim SU, Kim M, Lee SK, Roh J-K. Cyclooxygenase-2 inhibitor, celecoxib, inhibits the altered hippocampal neurogenesis

with attenuation of spontaneous recurrent seizures following pilocarpine-induced status epilepticus. Neurobiol Dis. 2006; 23:237–246. [PubMed: 16806953]

Kral T, Erdmann E, Sochivko D, Clusmann H, Schramm J, Dietrich D. Down-regulation of mGluR8 in pilocarpine epileptic rats. Synapse. 2003; 47:278–284. [PubMed: 12539201]

Kron MM, Zhang H, Parent JM. The developmental stage of dentate granule cells dictates their contribution to seizure-induced plasticity. J Neurosci. 2010; 30:2051–2059. [PubMed: 20147533]

Liu Y-B, Lio PA, Pasternak JF, Trommer BL. Developmental changes in membrane properties and postsynaptic currents of granule cells in rat dentate gyrus. J Neurophysiol. 1996; 76:1074–1088. [PubMed: 8871221]

Lothman EW, Stringer JL, Bertram EH. The dentate gyrus as a control point for seizures in the hippocampus and beyond. Epilepsy Res Suppl. 1992; 7:301–313. [PubMed: 1334669]

Marti-Subirana A, Soriano E, Garcia-Verdugo JM. Morphological aspects of the ectopic granule-like cellular populations in the albino rat hippocampal formation: a Golgi study. J Anat. 1986; 144:31–47. [PubMed: 2447048]

Masukawa LM, Uruno K, Sperling M, O'Connor MJ, Burdette LJ. The functional relationship between antidromically evoked field responses of the dentate gyrus and mossy fiber reorganization in temporal lobe epileptic patients. Brain Res. 1992; 579:119–127. [PubMed: 1623399]

McCloskey DP, Hintz TM, Pierce JP, Scharfman HE. Stereological methods reveal the robust size and stability of ectopic hilar granule cells after pilocarpine-induced status epilepticus in the adult rat. Eur J Neurosci. 2006; 24:2203–2210. [PubMed: 17042797]

Morgan RJ, Soltesz I. Nonrandom connectivity of the epileptic dentate gyrus predicts a major role for neuronal hubs in seizures. Proc Natl Acad Sci U S A. 2008; 105:6179–6184. [PubMed: 18375756]

Nadler JV. The recurrent mossy fiber pathway of the epileptic brain. Neurochem Res. 2003; 28:1649–1658. [PubMed: 14584819]

Nadler, JV. Axon sprouting in epilepsy. In: Schwartzkroin, PA., editor. Encyclopedia of basic epilepsy research. Elsevier; Oxford, UK: 2009. p. 1143-1148.

Nadler JV, Perry BW, Gentry C, Cotman CW. Loss and reacquisition of hippocampal synapses after selective destruction of CA3-CA4 afferents with kainic acid. Brain Res. 1980; 191:387–403. [PubMed: 7378766]

Okazaki MM, Evenson DA, Nadler JV. Hippocampal mossy fiber sprouting and synapse formation after status epilepticus in rats: visualization after retrograde transport of biocytin. J Comp Neurol. 1995; 352:515–534. [PubMed: 7721998]

Okazaki MM, Nadler JV. Glutamate receptor involvement in dentate granule cell epileptiform activity evoked by mossy fiber stimulation. Brain Res. 2001; 915:58–69. [PubMed: 11578620]

Okazaki MM, Molnár P, Nadler JV. Recurrent mossy fiber pathway in rat dentate gyrus: synaptic currents evoked in presence and absence of seizure-induced growth. J Neurophysiol. 1999; 81:1645–1660. [PubMed: 10200201]

Overstreet-Wadiche LS, Westbrook GL. Functional maturation of adult-generated granule cells. Hippocampus. 2006; 16:208–215. [PubMed: 16411232]

Parent JM, Yu TW, Leibowitz RT, Geschwind DH, Sloviter RS, Lowenstein DH. Dentate granule cell neurogenesis is increased by seizures and contributes to aberrant network reorganization in the adult rat hippocampus. J Neurosci. 1997; 17:3727–3738. [PubMed: 9133393]

Parent JM, Elliott RC, Pleasure SJ, Barbaro NM, Lowenstein DH. Aberrant seizure-induced neurogenesis in experimental temporal lobe epilepsy. Ann Neurol. 2006; 59:81–91. [PubMed: 16261566]

Patrylo PR, Dudek FE. Physiological unmasking of new glutamatergic pathways in the dentate gyrus of hippocampal slices from kainate-induced epileptic rats. J Neurophysiol. 1998; 79:418–429. [PubMed: 9425210]

Pekcec A, Fuest C, Mühlenhoff M, Gerardy-Schahn R, Potschka H. Targeting epileptogenesis-associated induction of neurogenesis by enzymatic depolysialylation of NCAM counteracts spatial learning dysfunction but fails to impact epilepsy development. J Neurochem. 2008; 105:389–400. [PubMed: 18194217]

Perrault P, Avoli M. Physiology and pharmacology of epileptiform activity induced by 4-aminopyridine in rat hippocampal slices. J Neurophysiol. 1991; 65:771–785. [PubMed: 1675671]

Pierce JP, Melton J, Punsoni M, McCloskey DP, Scharfman HE. Mossy fibers are the primary source of afferent input to ectopic granule cells that are born after pilocarpine-induced seizures. Exp Neurol. 2005; 196:316–331. [PubMed: 16342370]

Racine RJ. Modification of seizure activity by electrical stimulation. II. Motor seizure. Electroencephalogr Clin Neurophysiol. 1972; 32:281–284. [PubMed: 4110397]

Ribak CE, Seress L, Amaral DG. The development, ultrastructure and synaptic connections of the mossy cells of the dentate gyrus. J Neurocytol. 1985; 14:835–857. [PubMed: 2419523]

Ribak CE, Tran PH, Spigelman I, Okazaki MM, Nadler JV. Status epilepticus-induced hilar basal dendrites on rodent granule cells contribute to recurrent excitatory circuitry. J Comp Neurol. 2000; 428:240–253. [PubMed: 11064364]

Sanabria ERG, Su H, Yaari Y. Initiation of network bursts by Ca^{2+}-dependent intrinsic bursting in the rat pilocarpine model of temporal lobe epilepsy. J Physiol. 2001; 532:205–216. [PubMed: 11283235]

Santhakumar V, Aradi I, Soltesz I. Role of mossy fiber sprouting and mossy cell loss in hyperexcitability: a network model of the dentate gyrus incorporating cell types and axonal topography. J Neurophysiol. 2005; 93:437–453. [PubMed: 15342722]

Scharfman HE, Goodman JH, Sollas AL. Granule-like neurons at the hilar/CA3 border after status epilepticus and their synchrony with area CA3 pyramidal cells: functional implications of seizure-induced neurogenesis. J Neurosci. 2000; 20:6144–6158. [PubMed: 10934264]

Scharfman HE, Sollas AL, Goodman JH. Spontaneous recurrent seizures after pilocarpine-induced status epilepticus activate calbindin-immunoreactive hilar cells of the rat dentate gyrus. Neuroscience. 2002; 111:71–81. [PubMed: 11955713]

Scharfman HE, Sollas AE, Berger RE, Goodman JH, Pierce JP. Perforant path activation of ectopic granule cells that are born after pilocarpine-induced seizures. Neuroscience. 2003; 121:1017–1029. [PubMed: 14580952]

Schmidt-Hieber C, Jonas P, Bischofberger J. Enhanced synaptic plasticity in newly generated granule cells of the adult hippocampus. Nature. 2004; 429:184–187. [PubMed: 15107864]

Scimeni A, Schorge S, Kullmann DM, Walker MC. Epileptogenesis is associated with enhanced glutamatergic transmission in the perforant path. J Neurophysiol. 2006; 95:1213–1220. [PubMed: 16282203]

Shapiro LA, Ribak CE. Integration of newly born dentate granule cells into adult brains: hypotheses based on normal and epileptic rodents. Brain Res Rev. 2005; 48:43–56. [PubMed: 15708627]

Siebzehnrubl FA, Blümcke I. Neurogenesis in the human hippocampus and its relevance to temporal lobe epilepsies. Epilepsia. 2008; 49(Suppl 5):55–65. [PubMed: 18522601]

Sloviter RS, Zappone CA, Harvey BD, Bumanglag AV, Bender RA, Frotscher M. “Dormant basket cell” hypothesis revisited: relative vulnerabilities of dentate gyrus mossy cells and inhibitory interneurons after hippocampal status epilepticus in the rat. J Comp Neurol. 2003; 459:44–76. [PubMed: 12629666]

Spigelman I, Yan X-X, Obenaus A, Lee EY-S, Wasterlain CG, Ribak CE. Dentate granule cells form novel basal dendrites in a rat model of temporal lobe epilepsy. Neuroscience. 1998; 86:109–120. [PubMed: 9692747]

Stringer JL, Williamson JM, Lothman EW. Induction of paroxysmal discharges in the dentate gyrus: frequency dependence and relationship to afterdischarge production. J Neurophysiol. 1989; 62:126–135. [PubMed: 2754466]

Sutula T, Zhang P, Lynch M, Sayin U, Golarai G, Rod R. Synaptic and axonal remodeling of mossy fibers in the hilus and supragranular region of the dentate gyrus in kainate-treated rats. J Comp Neurol. 1998; 390:578–594. [PubMed: 9450537]

Tauck DL, Nadler JV. Evidence of functional mossy fiber sprouting in the hippocampal formation of kainic acidtreated rats. J Neurosci. 1985; 5:1016–1022. [PubMed: 3981241]

Thind KK, Ribak CE, Buckmaster PS. Synaptic input to dentate granule cell basal dendrites in a rat model of temporal lobe epilepsy. J Comp Neurol. 2008; 509:190–202. [PubMed: 18461605]

Thind KK, Yamawaki R, Phanwar I, Zhang G, Wen X, Buckmaster PS. Initial loss but later excess of GABAergic synapses with dentate granule cells in a rat model of temporal lobe epilepsy. J Comp Neurol. 2010; 518:647–667. [PubMed: 20034063]

Walter C, Murphy BL, Pun RYK, Spieles-Engemann AL, Danzer SC. Pilocarpine-induced seizures cause selective time-dependent changes to adult-generated hippocampal dentate granule cells. J Neurosci. 2007; 27:7541–7552. [PubMed: 17626215]

Zhan R-Z, Nadler JV. Enhanced tonic GABA current in normotopic and hilar ectopic dentate granule cells after pilocarpine-induced status epilepticus. J Neurophysiol. 2009a; 102:670–681. [PubMed: 19474175]

Zhan R-Z, Nadler JV. Activation of T-type calcium current underlies burst firing in hilar ectopic granule cells of epileptic brain. Soc Neurosci Abstr 39:#147.10. 2009b

Zhan R-Z, Timofeeva O, Nadler JV. High ratio of synaptic excitation to synaptic inhibition in hilar ectopic granule cells of pilocarpine-treated rats. J Neurophysiol. 2010; 104:3293–3304. [PubMed: 20881195]

Zhang X, Cui S-S, Wallace AE, Hannesson DK, Schmued LC, Saucier DM, Honer WG, Corcoran ME. Relations between brain pathology and temporal lobe epilepsy. J Neurosci. 2002; 22:6052–6061. [PubMed: 12122066]

Zhang W, Yamawaki R, Wen X, Uhl J, Diaz J, Prince DA, Buckmaster PS. Surviving hilar somatostatin interneurons enlarge, sprout axons, and form new synapses with granule cells in a mouse model of temporal lobe epilepsy. J Neurosci. 2009; 29:14247–14256. [PubMed: 19906972]

Zhao C, Teng EM, Summers RG, Ming G-L, Gage FH. Distinct morphological stages of dentate granule neuron maturation in the adult mouse hippocampus. J Neurosci. 2006; 26:3–11. [PubMed: 16399667]

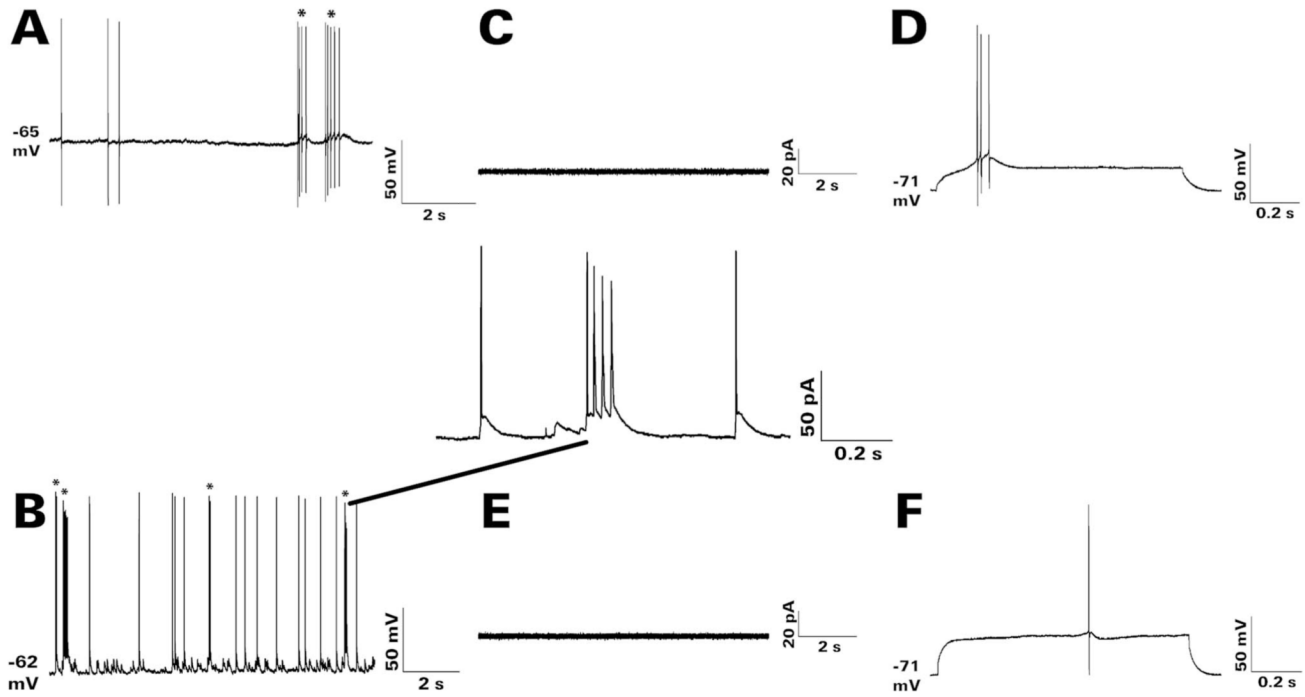

Figure 1.

Spontaneous and depolarization-evoked bursting of representative HEGCs. The recordings shown were obtained at 22-24 ° during superfusion at ≈3 mL/min with artificial cerebrospinal fluid that contained 122 mM NaCl, 25 mM $NaHCO_3$, 3.1 mM KCl, 1.8 mM $CaCl_2$, 1.2 mM $MgSO_4$, 0.4 mM KH_2PO_4, and 10 mM D-glucose, equlibrated with 95% O_2 / 5% CO_2. A cellular burst was defined as two or more action potentials superimposed on a single depolarizing wave. No such events were detected in recordings from any GC-SE or CGC made under these conditions. Cellular bursts are indicated by asterisks (*) in panels A, B. **A**: Gramicidin perforated patch recording in current clamp mode. Spontaneous action potentials and cellular bursts were recorded at the resting membrane potential of −65 mV. **B**: Whole-cell patch clamp recording in current clamp mode obtained soon after break-in. Spontaneous action potentials and bursts were recorded at the resting membrane potential of −62 mV. The expanded trace shows the fourth spontaneous burst in greater detail. **C,D**: Depolarization-evoked burst recorded during whole-cell patch clamp recording in current clamp mode. C: Membrane currents were monitored for 5 minutes during cell-attached recording in voltage clamp mode at a holding potential of −70 mV. No currents associated with spontaneous bursting were recorded from this cell. D: After achieving whole cell access, membrane potential was monitored during successive injections of depolarizing current from −0.5 to +1.9 nA for 1 second each. The cell's minimal response was a burst of action potentials first recorded during depolarization to −56 mV from a resting membrane potential of −71 mV. **E,F**: Lack of depolarization-evoked bursting in another recorded HEGC. E: Again, no currents associated with spontaneous bursting were observed by cell-attached recording. In addition, no spontaneous bursts were recorded at the resting membrane potential upon achieving whole cell access. F: Depolarization of this cell to −56 mV from a resting membrane potential of −71 mV evoked no response. Its minimal response was a single action potential first recorded during depolarization to −43 mV. In these respects, this nonbursting HEGC resembled closely all recorded GC-SEs and CGCs. CGC, normotopic granule cell from control rat; GC-SE, normotopic granule cell from rat that had

experienced status epilepticus; HEGC, hilar ectopic granule cell from rat that had experienced status epilepticus.

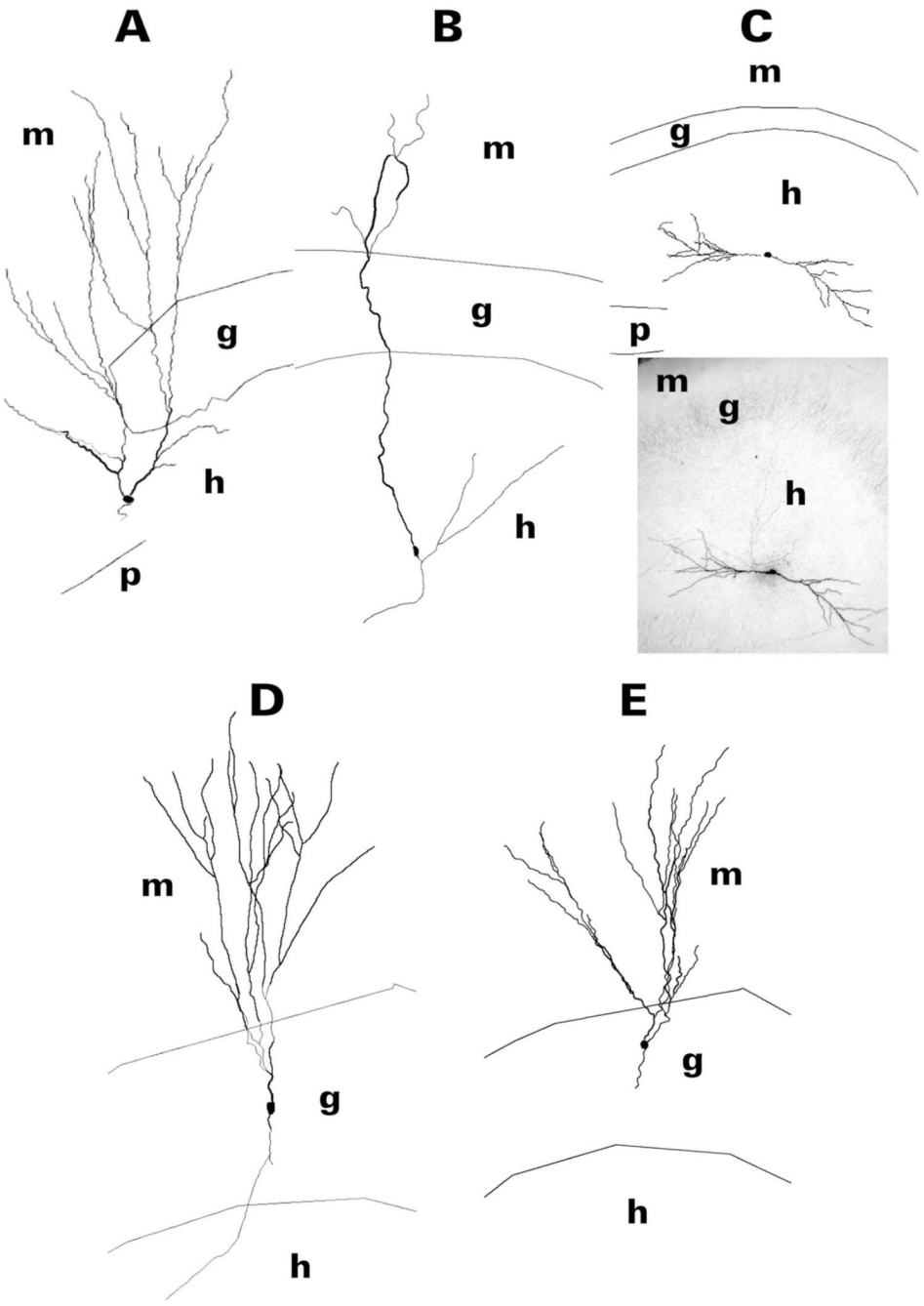

Figure 2.

Reconstruction of dentate granule cell somatodendritic morphology after filling the cell with biocytin during whole-cell patch clamp recording in hippocampal slices. After visualization of biocytin with avidin/horseradish peroxidase/diaminobenzidine, cells were reconstructed from serial sections with use of Neurolucida. Granule cells shown are representative of those cells having a hilar basal dendrite. HEGCs shown (**A–C**) were chosen to illustrate differences in the relative sizes of the apical and basal dendritic trees: predominantly apical (A), mainly apical (B), and apical and basal about equal (C). The apical dendrite of HEGCs could reach the outer edge of the dentate molecular layer (A,B) or be confined to the dentate hilus (C; the dendrite pointed to the left was considered the apical dendrite). Note the

relatively sparse branching of HEGC apical dendrites compared to those of GE-SEs (D) and CGCs (E) and the relatively exuberant branching of the distal apical dendrite(s) of GC-SEs compared to that of CGCs. A photomicrograph of the HEGC in panel C is included for comparison with the reconstruction. CGC, normotopic granule cell from control rat; g, granule cell body layer; GC-SE, normotopic granule cell from rat that had experienced status epilepticus; h, hilus of the dentate gyrus; HEGC, hilar ectopic granule cell from rat that had experienced status epilepticus; m, molecular layer of the dentate gyrus; p, pyramidal cell body layer of area CA3c.

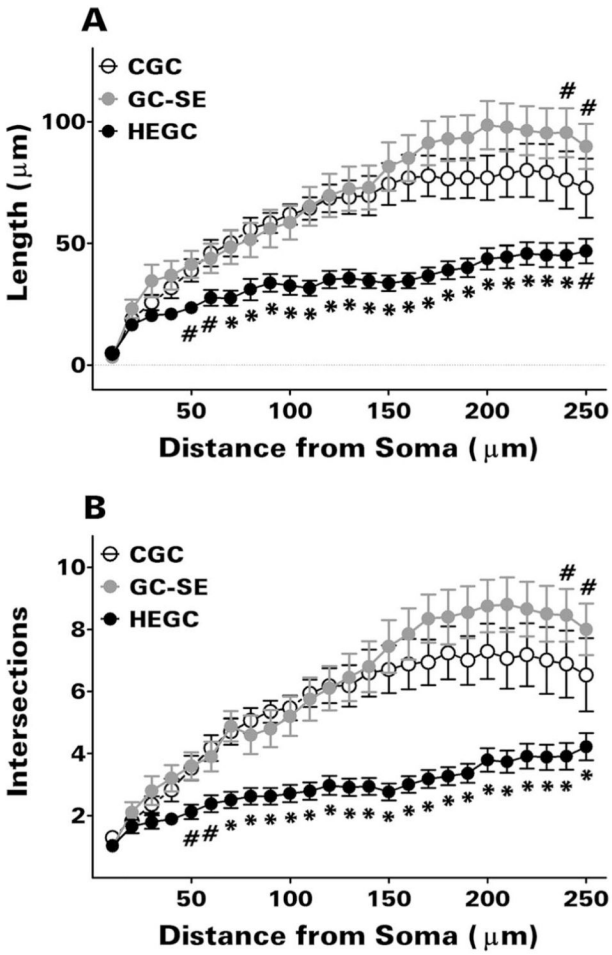

Figure 3.

Scholl analysis revealed significantly less apical dendritic length (**A**) and branching (**B**) in HEGCs than in normotopic granule cells beginning at 50 μm from the soma. This analysis also confirmed the greater length and branching of the distal apical dendrite in GC-SEs than in CGCs. Only HEGCs whose apical dendrite(s) penetrated through the dentate molecular layer were included. Values are means ± SEM for 34 HEGCs, 20 GC-SEs, and 17 CGCs. $^{\#}P$ <0.05 or $^{*}P$ < 0.01 compared with the other two groups by Newman-Keuls test after two-way ANOVA (granule cell group × dendritic segment) yielded P <0.001 for granule cell group, dendritic segment, and the interaction between these two variables. CGC, normotopic granule cells from control rats; GC-SE, normotopic granule cells from rats that had experienced status epilepticus; HEGC, hilar ectopic granule cells from rats that had experienced status epilepticus.

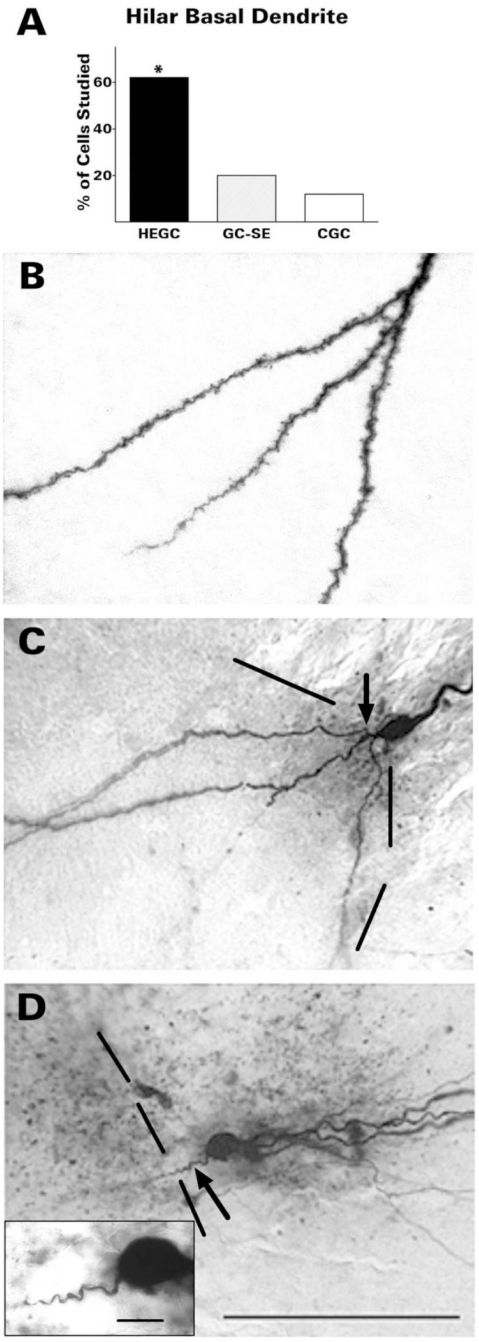

Figure 4.

HEGCs were much more likely to have a hilar basal dendrite than normotopic dentate granule cells (**A**). The hilar basal dendrite of HEGCs (**B**) was usually heavily invested with spines and branched either close to the soma, more distally, or both. The spiny hilar basal dendrite of GC-SEs (**C**) branched once close to the soma (arrow) or not at all. In contrast, the few basal dendrites observed on CGCs (**D**) were relatively short and unbranched, without visible spines (arrow). The inset in panel D illustrates the morphology of the CGC hilar basal dendrite at higher magnification. Dashed lines indicate the border between the granule cell body layer and hilus. Quantitative data were derived from microscopic

observation of 79 HEGCs, 54 GC-SEs, and 40 CGCs. *P <0.001 compared with the other two groups by χ-square test. CGC, normotopic granule cells from control rats; GC-SE, normotopic granule cells from rats that had experienced status epilepticus; HEGC, hilar ectopic granule cells from rats that had experienced status epilepticus. Scale bars 100 μm; inset, 10 μm.

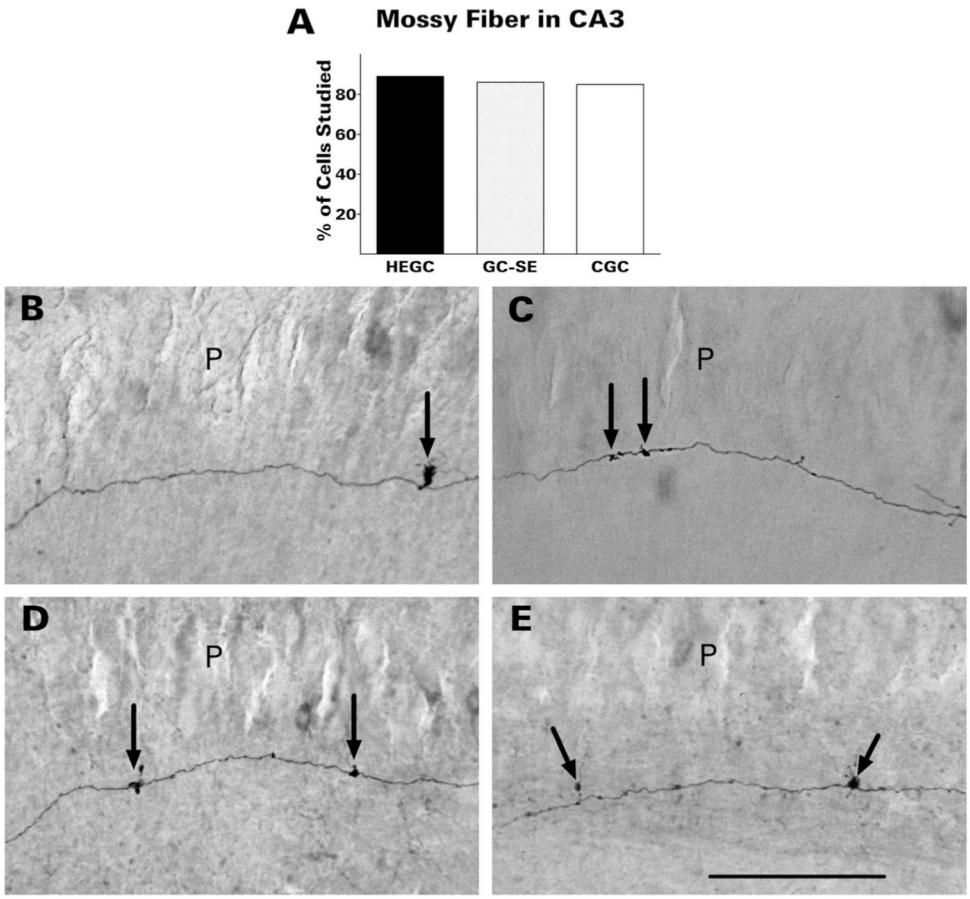

Figure 5.

HEGCs were about as likely as normotopic dentate granule cells to project to area CA3 neurons within the slice (**A**). Mossy fibers of HEGCs (**D,E**), like those of granule cells from control rats (**B**) and GC-SEs (**C**), had widely spaced giant boutons in stratum lucidum from which filopodia emerged (arrows). Quantitative data were derived from microscopic observation of 55 HEGCs, 32 GC-SEs, and 33 CGCs. CGC, normotopic granule cells from control rats; GC-SE, normotopic granule cells from rats that had experienced status epilepticus; HEGC, hilar ectopic granule cells from rats that had experienced status epilepticus; P, pyramidal cell body layer. Scale bar = 200 μm.

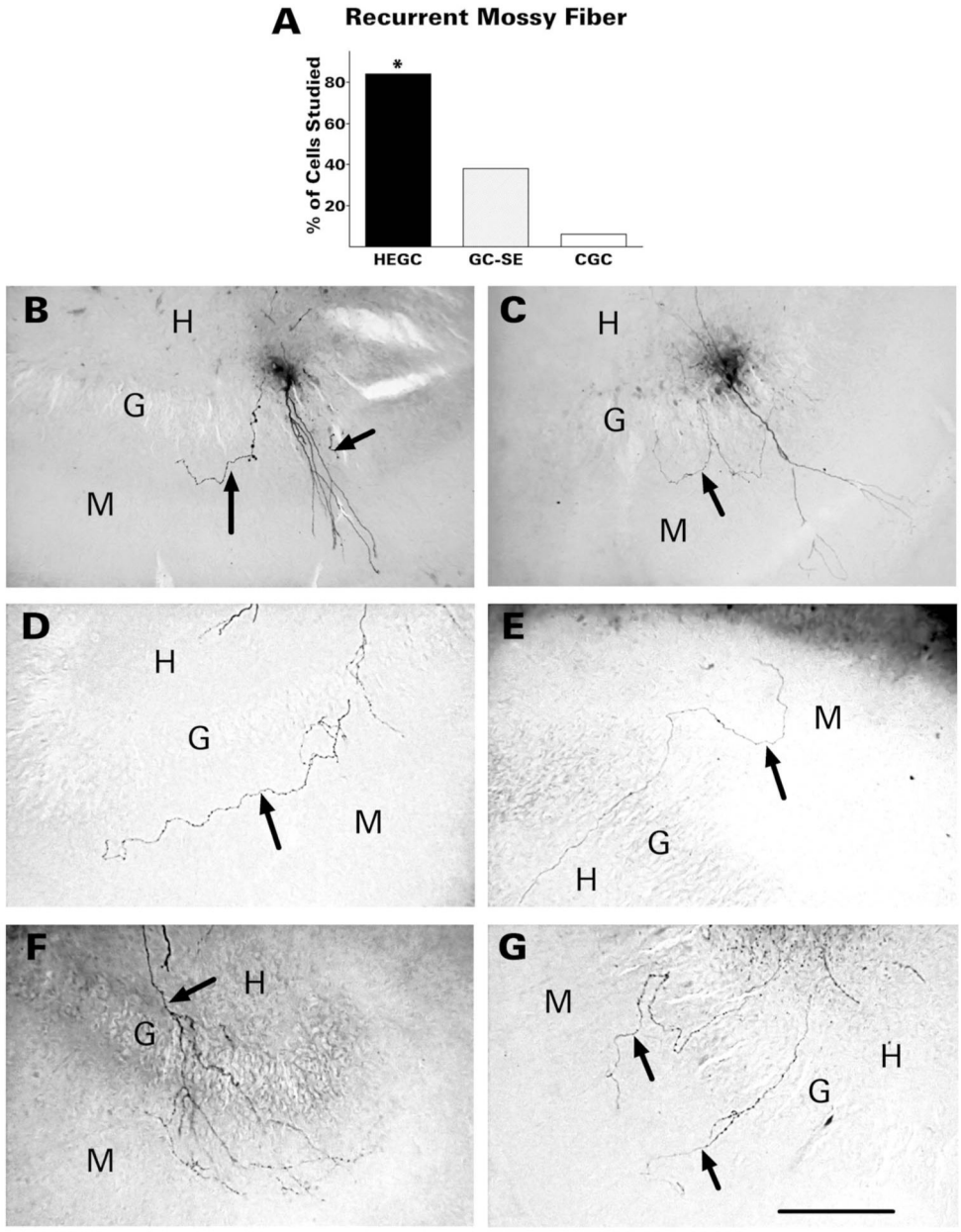

Figure 6.

HEGCs were much more likely to send one or more recurrent mossy fibers (arrows) into the dentate molecular layer than normotopic granule cells (A). B,C: Recurrent mossy fibers of GC-SEs. In panel B the labeled cell has two visible recurrent mossy fibers in the molecular layer, one of which courses through the inner third of the molecular layer parallel to the granule cell body layer. In panel C, one recurrent fiber branches in the granule cell body layer and the two branches course in opposite directions through the inner molecular layer. D-G: Recurrent mossy fibers of HEGCs. D: A single recurrent mossy fiber courses through the inner third of the molecular layer parallel to the granule cell body layer. E: The fiber runs for a short distance through the inner third of the molecular layer then extends through the outer part of the layer. F: A recurrent mossy fiber branches extensively in the granular and molecular layers. G: Two separate fibers emerge from the hilus and cross the granule

cell body layer. Quantitative data were derived from microscopic observation of 55 HEGCs, 32 GC-SEs, and 33 CGCs. *P <0.001 compared to the other two groups by χ-square test. CGC, normotopic granule cells from control rats; G, granule cell body layer; GC-SE, normotopic granule cells from rats that had experienced status epilepticus; H, hilus of the dentate gyrus; HEGC, hilar ectopic granule cells from rats that had experienced status epilepticus; M, molecular layer of the dentate gyrus. Scale bar = 200 μm.

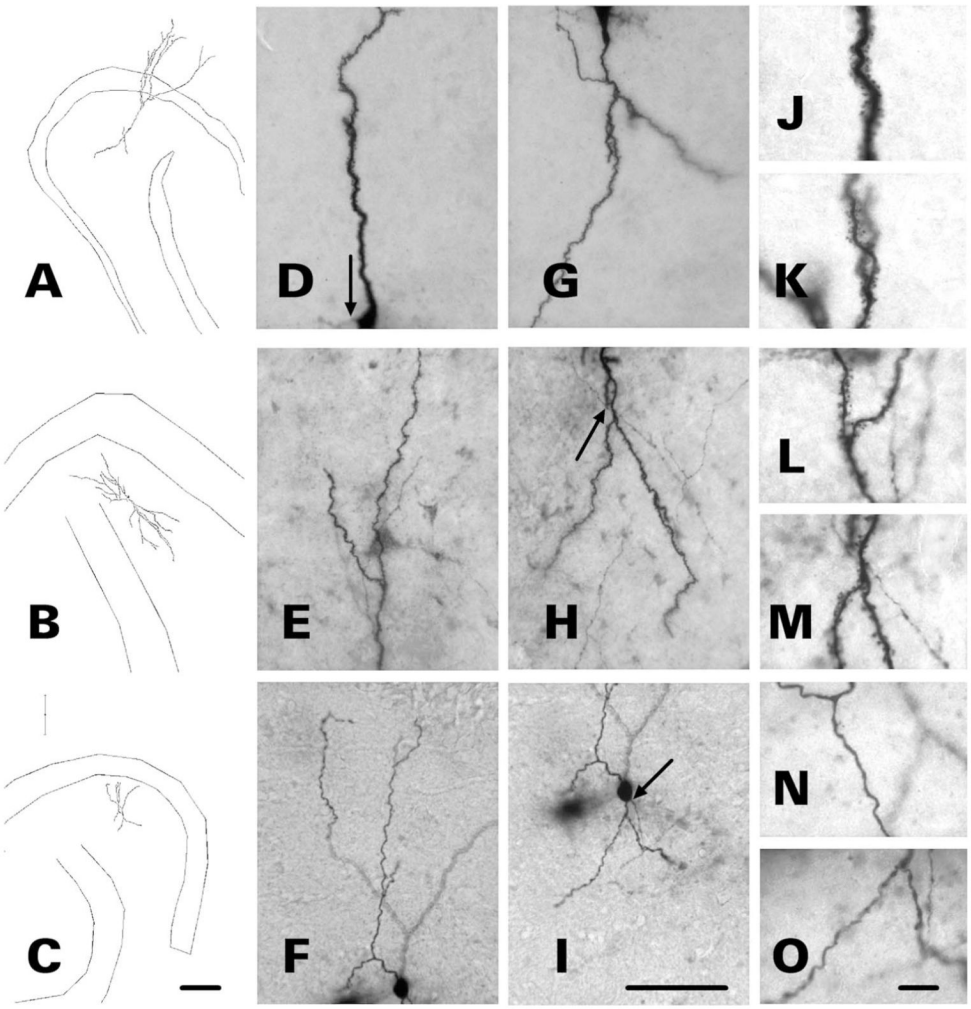

Figure 7.

Dendritic morphology of three bursting HEGCs. Cells were filled with biocytin during whole-cell patch clamp recording and cell morphology was reconstructed with use of Neurolucida. Micrographs of the apical (**D–F**) and basal (**G-I**) dendrites of the three representative HEGCs are shown to the right of each reconstruction (**A-C**). Arrows indicate the origin of the mossy fiber. The micrographs to the far right of each reconstruction illustrate the morphology of apical (**J,L,N**) and basal (**K,M,O**) dendrites at higher magnification. Dendrites of HEGC A exhibit morphology typical of both bursting and nonbursting HEGCs. The apical dendritic branches reach the outer edge of the molecular layer and both apical and hilar basal dendrites appear fully formed and heavily invested with spines. Dendrites of HEGC B are confined to the hilus, but dendritic structure appears normal otherwise. The varicose dendrites of HEGC C are confined to the hilus, are unusually short, and lack mature spines. Scale bars = 200 μm left; 70 μm center; 10 μm right.

TABLE 1
Dendritic Length and Branching of HEGCs and Normotopic Dentate Granule Cells

		Length (μm)	Branching (# of branch points)
Total (apical + basal)	HEGC - dendrite(s) in ML (*N* = 34)	21 13 (761-5225)	9 (1-18)
	HEGC - dendrite(s) confined to hilus (*N* = 10)	1577 (119-3167)	12 (1-20)
	GC-SE (*N* = 20)	2515 (1053-4584)	12 (7-22)
	CGC (*N* = 17)	1951 (998-3735)	10 (4-21)
Apical	HEGC - dendrite(s) in ML (*N* = 34)	1612 (464-5225)*	6 (1-17)*
	HEGC - dendrite(s) confined to hilus (*N* = 10)	999 (56-2854)**	6 (1-20)
	GC-SE (*N* = 20)	2458 (1016-4584)	12 (6-22)
	CGC (*N* = 17)	1879 (731-3735)	10 (4-21)
Basal	HEGC - dendrite(s) in ML (*N* = 26)	291 (8-2727)	2 (0-14)
	HEGC - dendrite(s) confined to hilus (*N* = 9)	358 (63-1909)	2 (0-11)
	GC-SE (*N* = 8)	125 (38-278)	1 (0-1)

Values were obtained from Scholl analysis of dentate granule cells labeled by intracellular dialysis with biocytin during whole cell patch clamp re cording. They are expressed as medians and (range) for the number of cells (*N*) indicated. HEGCs with one or two dendrites in the molecular layer were compared to GC-SEs and CGCs by the Kruskal-Wallis one-way ANOVA on ranks. HEGCs with dendrites confined to the hilus were compared to HEGCs with one or two dendrites in the molecular layer by the Mann-Whitney rank sum test.

* $P < 0.05$ compared to GC-SE by Dunn's test after Kruskal-Wallis one-way ANOVA on ranks yielded $P < 0.05$.

** $P < 0.05$ compared to HEGCs with dendrites in the molecular layer by Mann-Whitney rank sum test. CGC, normotopic granule cells from control rats; GC-SE, normotopic granule cells from rats that had experienced status epilepticus; HEGC, hilar ectopic granule cells from rats that had experi enced status epilepticus; ML, molecular layer of the dentate gyrus.

TABLE 2
Comparison of All Bursting and Nonbursting HEGCs Analyzed

	Bursting	Nonbursting
Total dendritic length (μm)	1256 (1 19–3171)**	2874 (1985–5226)
Total branching (# of branch points)	5 (2–17)**	15 (10–19)
Dendritic length in hilus (μm)	420 (48–1356)	361 (17–1013)
% of apical dendritic length in hilus	59 (1–100)	33 (1–100)
% of total dendritic length in hilus	55 (1–100)	25 (1–100)
Resting V_m (mV)	−66 ± 2	−71 ± 2
Input resistance (MΩ)	314 ± 31	249 ± 26

Morphological data were obtained from Scholl analysis of HEGCs labeled by intracellular dialysis with biocytin during whole cell patch clamp recording. Values are expressed as medians and (range) for 17 bursting and 7 nonbursting HEGCs.

** *P* <0.025 compared to non-bursting HEGCs by Mann-Whitney rank sum test. During whole cell recordings, resting V_m was determined in current clamp mode immediately on break-in. During perforated patch recordings, resting V_m was determined in current clamp mode when the series resistance fell below 20 MΩ. Input resistance was deter mined from the current response to a 10-mV hyperpolarization from resting V_m applied for 200 ms. Values are expressed as means ± SEM for 18 bursting and 8 nonbursting HEGCs.

TABLE 3

Dendritic Length and Branching of Bursting and Nonbursting HEGCs with Dendrites in the Molecular Layer

		Length (μm)	Branching (# of branch points)
Total (apical + basal)	Bursting	1393 (198–3172)*	4 (1–15)**
	Nonbursting	2910 (1985–5226)	14 (10–17)
Apical	Bursting	1111 (117–3172)*	3 (1–15)**
	Non-Bursting	2780 (1032–5226)	14 (6–17)
Basal	Bursting	223 (43–2727)	1 (0–4)
	Non-Bursting	291 (40–1380)	2 (0–7)

Values were obtained from Scholl analysis of dentate granule cells labeled by intracellular dialysis with biocytin during whole cell patch clamp recording. They are expressed as medians and (range) for 12 bursting and 6 nonbursting HEGCs with one or two apical dendrites in the dentate molecular layer.

* $P < 0.05$,

** $P < 0.025$ compared to nonbursting HEGCs by Mann-Whitney rank sum test.